Construction and Building Materials 105 (2016) 579–588

Contents lists available at ScienceDirect

Construction and Building Materials

journal homepage: www.elsevier.com/locate/conbuildmat

Performance of unprotected and protected cellular beams in fire conditions

Ali Nadjai [a,*], Klelia Petrou [b], Sanghoon Han [a], Faris Ali [a]

[a] University of Ulster, School Built Environment, FireSERT, Shore Road, Newtownabbey, Co-Antrim BT37 0QB, Northern Ireland, United Kingdom
[b] Hoare Lea, Western Transit Shed, 12-13 Stable Street, London NIC 4AB, United Kingdom

HIGHLIGHTS

- Experimental study of cellular steel beams in fire conditions.
- Comparaison of unprotected and protected cellular steel beams.
- Failure mechanism and numerical modelling.
- Design apparoach and eurocode comparaison.

ARTICLE INFO

Article history:
Received 4 April 2015
Received in revised form 27 November 2015
Accepted 22 December 2015
Available online 4 January 2016

Keywords:
Cellular beams
Intumescent coating
Fire resistance
Finite element method

ABSTRACT

This paper describes an experimental study at elevated temperatures on the behaviour of full-scale composite floor unprotected and protected cellular steel beams with intumescent coating having different size and openings shape. All beams were designed for a full shear connections between the steel beam and the concrete flange using headed shear studs in order to fail in by web-post buckling. In fire, the temperature distribution across a composite member is non-uniform, since the web and bottom flange have thin cross-sections and a greater exposed perimeter than the top flange. The deterioration of the material properties of the web will therefore become an important effect on the overall performance of the member in the event of fire. Fire resistance and protection of cellular beams has been very controversial concerning their behaviour in elevated temperatures, the fire protection material and the required thickness. Two failure temperatures were observed in the fire tests indicated that cellular beams failed by web post buckling and Vierendeel bending associated with the buckling of the web posts of the steel section. The finite element modelling software TNO-Diana was used to complete the numerical investigation. Comparison of the experimental and FEM results is presented and both are in good agreement. However the Euro code approach can be improved by using the correct material specification of the intumescent coating used.

1. Introduction

Cellular beams give architectural flexibility having open large spaces forming compartments, as it is possible to achieve long spans. This structural element is currently being widely used in multi-storey buildings, commercial and industrial buildings, warehouses and portal frames, in the UK and Europe. The investigation of cellular beams at ambient temperature was well covered by various studies on theoretical, experimental and finite element schemes [1–3]. As a results a number of different failure modes have been observed. In fire, the degradation of strength and stiffness of unprotected steel sections exposed to elevated temperatures can result to early structural collapse [4–6]. The fire resistance of cellular beams has been very controversial in the recent years, considering the fire protection material and the required thickness in a number of guidelines documents published by the Steel Construction Institute [7,8]. The most common fire protection material used for cellular beams is the intumescent coating, giving the advantage of allowing the passage of technical services as it can be applied without blocking the holes in the web. Intumescent coating is applied on steel structural elements at specific thickness, necessary to protect the structural element, minimising the wastage and hence cost. They can be applied in the fabricator's shop or on the completed structure on the con-

* Corresponding author.
E-mail addresses: a.nadjai@ulster.ac.uk (A. Nadjai), petrou.klelia@gmail.com (K. Petrou).

http://dx.doi.org/10.1016/j.conbuildmat.2015.12.150
0950-0618/

struction site. In addition, ensures that the steel work is fully fire protected throughout the construction phase. Intumescent coatings contain a mixture of chemical ingredient, reactive in fire conditions producing an insulating layer of carbonaceous char. They can be swelling to between 5 and 50 times their original applied thickness, so that 1 mm film can produce up to 50 mm of char [9]. The char contains air vacuoles in a carbon based matrix, which effectively surrounds and insulated the steel substrate from the rapid temperature increase that will occur to an unprotected steel section.

The use of intumescent coating extends the loadbearing capacity of the steel structure. The stability of a building, having intumescent coating protected steel structural elements, in case of fire depends on the thickness of the coating, the depth and insulation properties of the char produced of it [9,10].

2. Expiremental procedure

The experimental work is a continuation of the research fire test programme funded by the EPSRC and conducted at the University of Ulster, FireSERT Laboratory. The tests carried out on six full-scale composite unprotected and protected cellular beams, of 5 m span length. The cellular beams were fabricated from standard hot-rolled steel sections, subjected to one or two point loading, using three different geometries.

2.1. Beam detail information

The following types of beams provided in Table 1 and shown in Fig. 1 have been tested: (a) beam 1: an asymmetric composite cellular beam, having large web opening, was produced on the basis of UB 356 × 171 × 57 as a top tee section and of UB 610 × 305 × 179 as a bottom tee section having finished depth of 555 × 171/305ACB × 118 kg/m. The diameter of cells was 375 mm at 600 mm centers; (b) beam 2: a symmetrical composite cellular beam, having two large web openings, was produced on the basis of UB 457 × 191 × 74, having a finished depth of 550 × 191CB74 kg/m. The cells diameter was 335 mm at 600 mm centers; (c) beam 3: an asymmetrical composite cellular beam, having multiple circular web openings, was produced on the basis of UB 356 × 171 × 57 as a top tee section and of UB 457 × 191 × 74 as a bottom tee section having finished depth of 555 × 171/191ACB × 65.5 kg/m. The cells diameter was 375 mm at 600 mm centers.

Table 1
Geometry data.

	Beam 1	Beam 2	Beam 3
Span (mm)	4500	4500	4500
Top flange-w/t (mm)	172.2/13.0	190.4/14.5	172.2/13.0
Top tee depth (mm)	255	275	255
Bottom flange-w/t (mm)	307.1/23.6	190.4/14.5	190.4/14.5
Bottom tee depth (mm)	300	275	300
Web thickness-top/btm (mm)	8.1/14.1	9.0/9.0	8.1/9.0
Overall depth (mm)	555	550	555
Number of circular cells	6	2	6
Number of elongated cells	1	2	0
Number of cellswith infill	0	1	1
No. of cells with semi infill	2	0	0
Overall number of cells	7	5	7
Cell diameter (mm)	375	335	375
Cell spacing (mm)	600	600	600

The cellular beams were S355 steel grade. In the six fire tests was used a 150 mm thick × 1100 mm wide concrete slab, of normal weight concrete, grade 35 N/mm^2. The reinforcement consisted of welded wire mesh A142 of 460 N/mm^2 yield strength. The interaction between slab and beam was ensured in all specimens with shear connectors of 19 mm diameter studs at height 95 mm. They have been equally distributed in one row with a distance of 150 mm over the beam length. The steel deck was Multideck 50-V2 of strength 350 N/mm^2, having 0.9 mm thickness. Concrete compressive strength was determined at different stages of time: after 2 weeks, 28 days and during the testing days giving an average of 35 N/mm^2 using a compressive strength calibrated machine at the University of Ulster.

2.2. Intumescent coating

For fire protection of the cellular beams was used the intumescent coating material Nullfire S707-60. Experienced engineers from the company that provided the material conducted the application of the intumescent coating. The process was completed in three stages as illustrated in Fig. 2, primer coating was applied along the openings, next it was applied along the full length of the cellular beams and finally the intumescent coating was applied. The thickness of both layers was measured carefully along the whole procedure making sure the final thickness meets the required thickness for providing 60 min fire protection. Final intumescent coating thickness for composite cellular beam 1 was, 605 (μm), for composite cellular beam 2, 586 (μm) and composite cellular beam 3, 637 (μm).

2.3. Mechanical and thermal loading

Composite cellular beam 1 was tested under two-points loading and the other 2 beams were tested under one point loading; both ends of the beams were simply supported. The cellular beams were designed at ambient temperature in order to determine the failure load. The loading was considered nearly equal to 30% of the ultimate load found from the pre-design at cold conditions and by taken into account the previous tests conducted at University of Ulster as Ref. [11].

In order to evaluate the fire resistance of the protected cellular beams the applied loading in protected and unprotected composite cellular beam tests were kept the same. The applied load for cellular beam 1 was 200 kN and 150 kN for cellular beam 2 and cellular beam 3.

The fire load was represented by the standard ISO 834 fire curve. Exposed to fire was the lower side of the composite slab and the steel section.

Temperature distribution on the composite cellular beams was recorded by thermocouples disposed at various locations along the cellular beam in different zone and by 10 thermocouples disposed along the composite slab. Fig. 3 demonstrates the typical thermocouples locations used for the cellular beams. Deflections and axial displacements were recorded using 5 Linear Differential Transducers LVDT's, placed in different location on the unexposed concrete slab.

All beams were kept loaded to their respective applied load for duration over an hour time before the furnace started functioning. The positions of the thermocouples (Fig. 3) were located at each web post along its depth of the section, around the openings and also trough the slab cross-sections. The six fire tests for unprotected and protected cellular beams were carried out under the ISO 834 fire curve. Only the lower side of the slab and the steel section were fire-exposed.

3. Fire tests and results

3.1. Unprotected beams

The average temperatures distribution along the steel profile of the three unprotected beams is shown in Fig. 4. The average tem-

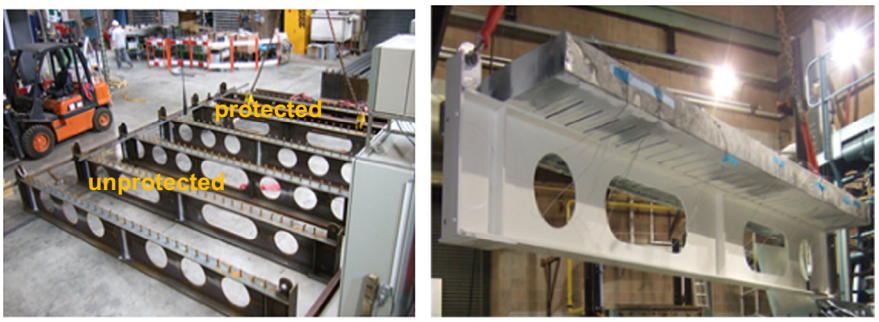

Fig. 1. Steel cellular beams with different opening shapes.

Fig. 2. Intumescent coating application procedure.

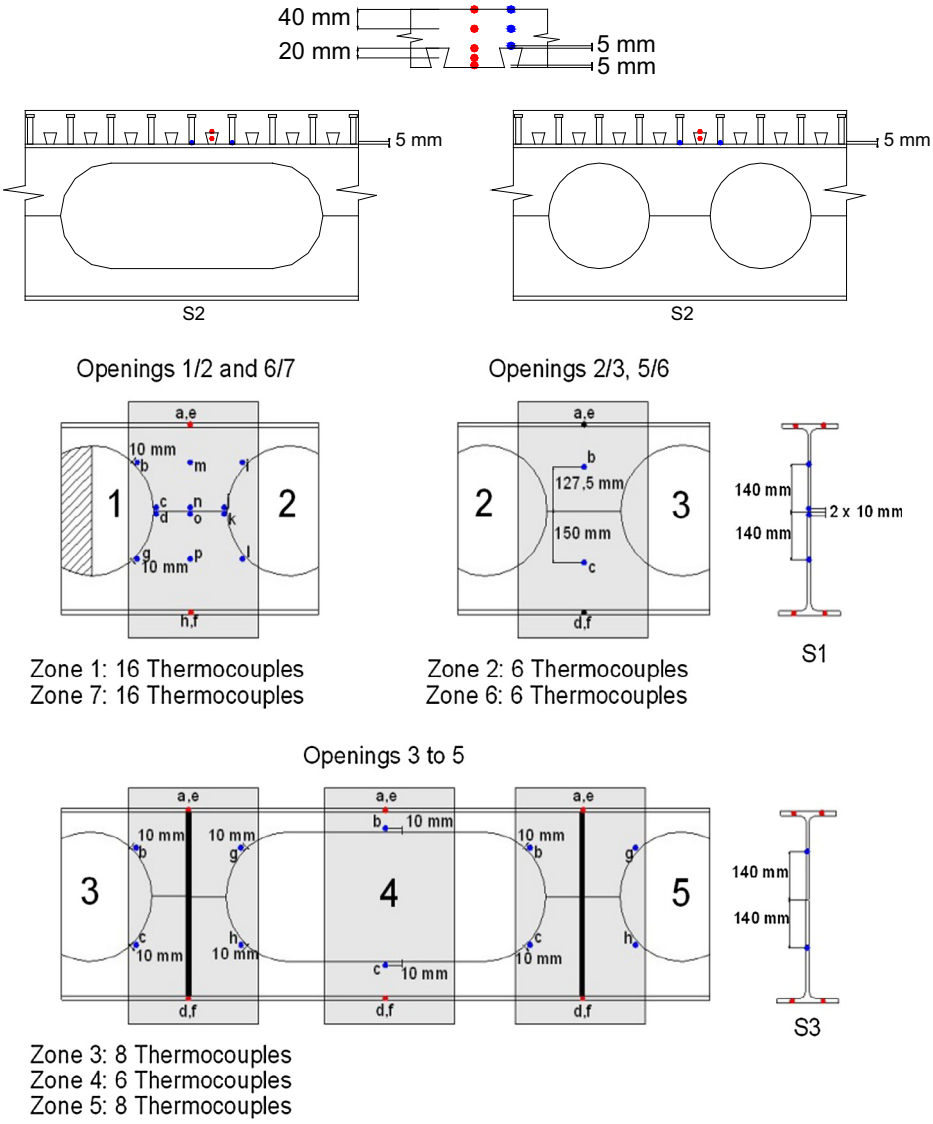

Fig. 3. Typical thermocouple positions in cellular tested beams and concrete slab cross-sections.

peratures of top flanges are the coldest part of the steel beams cross section with a significant thermal gradient due to the influence of the slab (Fig. 5). The maximum temperature values were recorded in the web, reaching up to 795 °C in beam 2 after 39 min (Fig. 4). The beam responded linearly due to the severe rise in temperature until about 20 min by which time the furnace temperature has risen to over 730 °C. After this point the beam rate of deflection begins to gradually increase due to the deterioration of the beam properties until about 24 min when the beam deflection is recorded at furnace temperature around 800 °C. Between 20 and 25 min time, beam 2 rate of deflection starts to increase rapidly until the point of failure at 39 min by which time the beam have deflected by 249 mm at furnace temperature around 870 °C. In the case of the ISO 834 fire, there is no time for significant heat

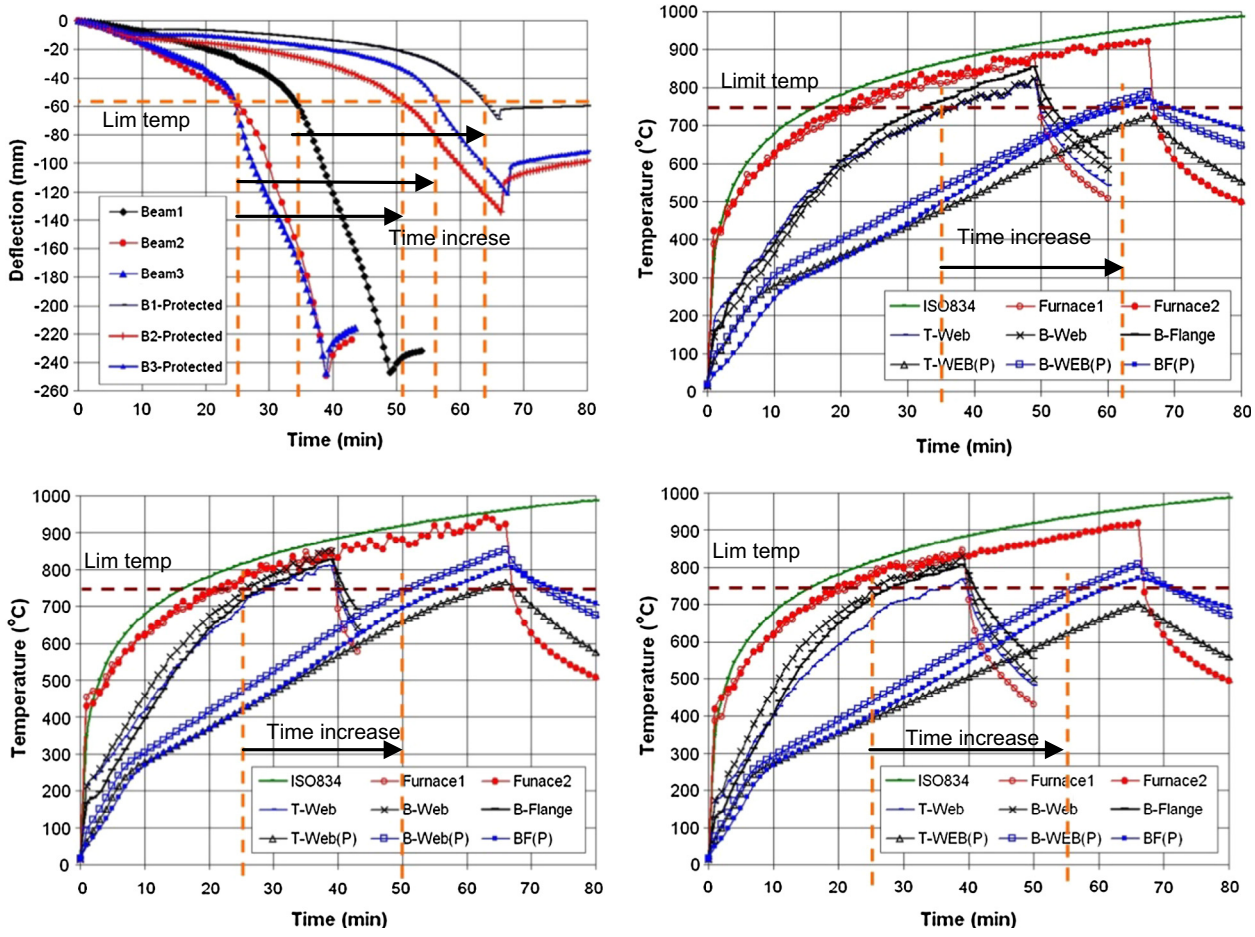

Fig. 4. Deflections and temperatures distribution on protected and unprotected cellular beams.

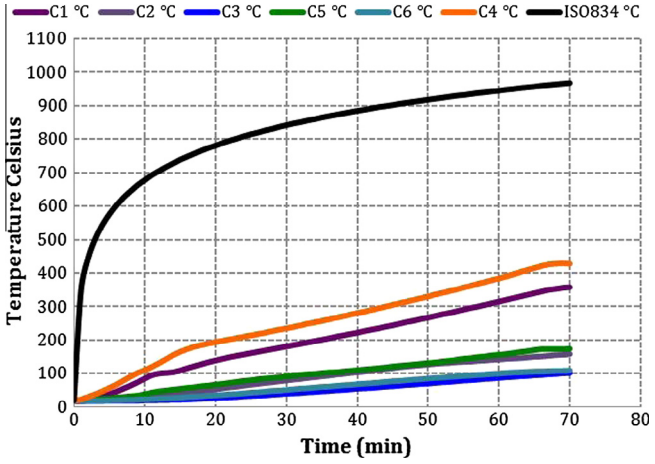

Fig. 5. Temperature distribution through the concrete slab.

to be conducted through the concrete slab so there is less of a restraining force generated and the deflection rises rapidly. It can be deduced from this that the main reason for failure occurring is due to the loss of the steel strength and stiffness rather than a combined loss of material property in the steel and concrete.

3.2. Protected beams

Fig. 4 demonstrates the results of recoded deflections and temperatures distribution through the steel sections compared with the unprotected similar beams. The maximum-recorded temperatures on the protected composite cellular beams were in the bottom web of the steel sections. At time 66 min when the furnace test stopped the maximum temperatures were 787 °C, 837 °C, 798 °C for B1, B2 and B3 respectively (Table 2). The temperature distribution inside the concrete slab (Fig. 5) remains cooler compared to the steel cellular beams (Fig. 4). The maximum recorded temperature was at the bottom of the slab of 429 °C at 69 min and minimum temperaures near the surface of the concrete slab of 101 °C.

The protected composite cellular beams failed in longer time than the unprotected and the recorded deflection at failure time was less than the unprotected. Temperature distribution and deflections results confirmed the effectiveness and importance of applying fire protection on cellular beams. It can be seen from Fig. 4 that protection results in increase of time fire resistance of all protected beam up to 50% compared with unprotected beams when the temperature is 750 °C for time limit of 60 min as provided by the manufacturer.

Table 2
Experimental results, temperature distribution.

Cellular beam section	B1 (66 min)	B2 (66 min)	B3 (66 min)
Top flange	520	502 °C	473 °C
Top web	720 °C	754 °C	694 °C
Bottom web	787 °C	839 °C	798 °C
Bottom flange	769 °C	811 °C	771 °C

Table 3
Experimental Deflections and temperatures at 30, 60 and 66 min of fire exposure.

Cellular beams	Time 30 min	Time 60 min	Time 66 min
B1 Def (mm)	10	42.3	73.1
B1 Temp (°C)	489	751	787
B2 Def (mm)	21.7	102.15	132.01
B2 Temp (°C)	514	798	838
B3 Def (mm)	14.9	86.78	117.94
B3 Temp (°C)	454	756	798

3.3. Recorded deflections

A comparison on the recorded mid-span deflections of protected and unprotected composite cellular beams reveals and confirms the effectiveness of fire protection as presented in Fig. 4. The deflection on the unprotected composite cellular beams increased linearly after 20 min exposure to ISO-834 curve, when the average furnace temperature is higher than 800 °C. After 20 min the rate of deflection increased rapidly until failure at 45 min for composite unprotected cellular beam 1 and at 39 min for composite unprotected cellular beams 2 and 3, after the fire test started. On the other hand, the protected for 60 min composite cellular beams, had a linear response of mid-span deflection until 30 min after the start of the fire test, after this time step transform to nonlinear. Table 3 shows the recorded temperatures for bottom web for each cellular beam at same times of exposure. It can be concluded that the resulted deflections are a consequence of the temperatures increase across the cellular beams. Due to the heated steel section the degradation of the material properties, yield strength $f_y(\theta)$, and young module $E(\theta)$, lead to the displacement and finally failure of the cellular beams. At 60 min fire exposure, which is the fire protection limit time provided by the applied intumescent coating, the resulted temperatures are higher than 750 °C. In addition, at the stopping time of the fire tests, 66 min the higher temperatures achieved are close to 800 °C.

Considering the geometry and size of the composite cellular beams, the recorded mid-span deflections on the symmetric protected cellular beam 2 are higher than the other two asymmetric cellular beams (see Table 3). Hence, the effect of elevated temperatures on composite protected symmetric cellular beam 2 materials is more intense than the other two asymmetric beams.

Recorded temperature and mid-span deflection (Fig. 4) comparison for protected and unprotected composite cellular beams demostrated the necessity of fire protection of cellular beams with intumescent coatings, increasing their life time and ability on holding the load, when exposed to severe fire conditions. The heat transfer through the concrete slab, during the fire exposure was not significant, as illustrated in Fig. 5, with highest temperatures less than 450 °C. Thus, it is presumed that the main reason for failure occurring is due to the loss of the steel strength and stiffness rather than a combined loss of material properties in the steel and concrete.

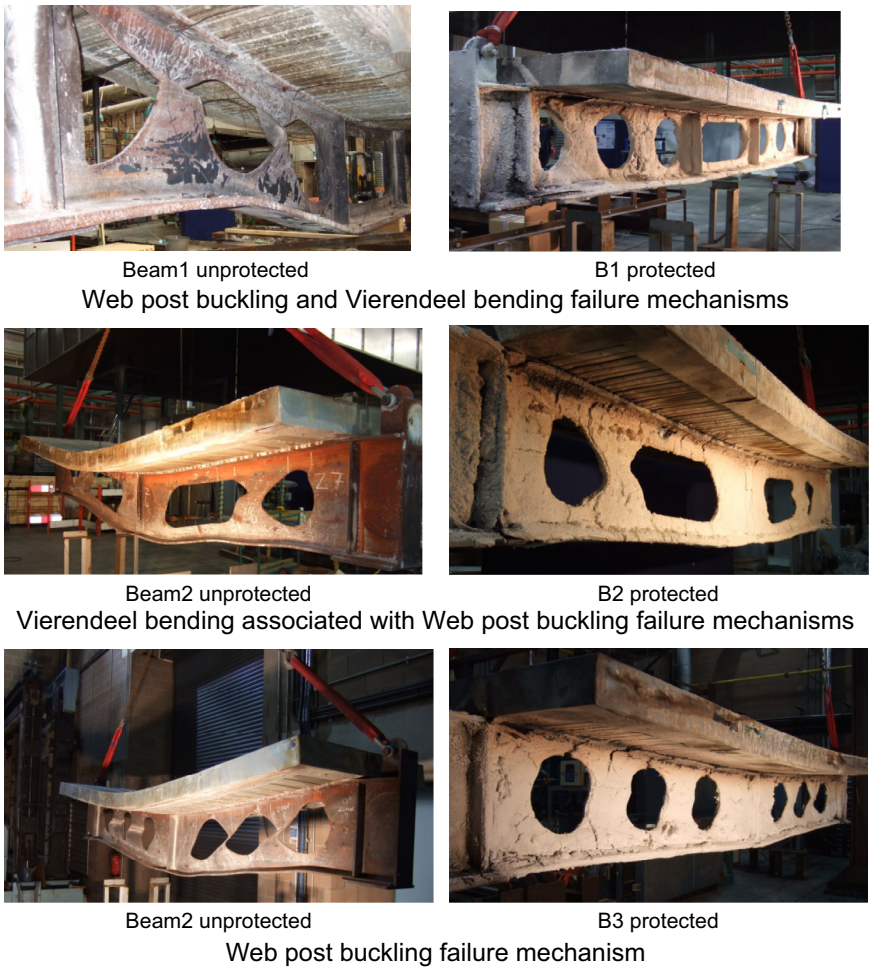

Fig. 6. Failure mechanism of the unprotected and protected cellular beams.

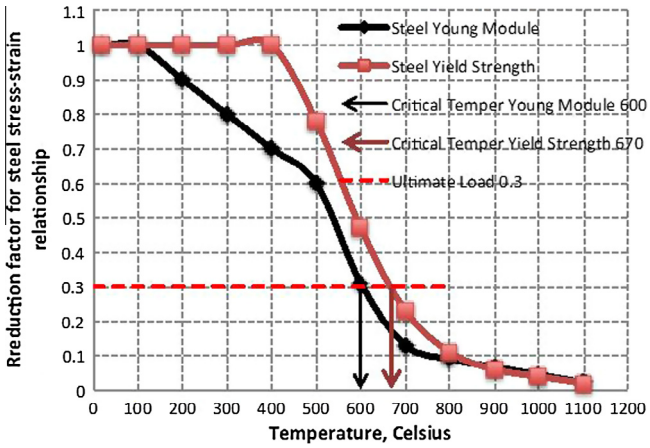

Fig. 7. Young Modulus and yield critical temperatures for 0.3 ultimate factors.

3.4. Failure mechanisms

Unprotected cellular beams: the temperature difference between the top and bottom flange was observed to be greater due to the significant rise in furnace temperature in the case of the ISO fire, but it was not relevant for the web post buckling. However, buckling of the web posts begins to occur before the final point of failure as the steel beam temperatures are in excess of 600 °C at which point the steel has less than half of its design strength and Young's modulus is reduced to 20%. When the furnace temperature is around 750 °C, the Young's modulus decreases quicker than the steel strength limit; which may causes the failure modes. The main failure mode in beam 1 and beam 2 was the Vierendeel bending associated with the buckling of the web posts of the steel section. The web post buckling was the main failure mode in the beam 3. More information about unprotected beams in fire are provided in Ref. [11].

Protected cellular beams: taking the protected cellular beams out from the furnace chamber, first observation was the swelling of intumescent coating, creating the char instead of the original paint form, as illustrated in Fig. 6. Closer observations on the specimens lead to the identification of the failure modes. Web-post buckling dominates the cellular beams failure as a result of the temperature difference between bottom and top flange. On the asymmetric cellular B1 the web-post buckling is located only on the solid web close to the supported edges, Fig. 6. Also, is not clear if Vierendeel bending action was appeared before the web-post buckling. Vierendeel bending in combination with the web-post buckling can be indicated on cellular B2 web between circular and elongated opening, Fig. 6. Asymmetric cellular B3 has failed due to web-post buckling located between the circular openings along the span, Fig. 6.

Eurocode 3 [12], provides the reduction factors of yield strength and Young Modulus for steel sections, when exposed to elevated temperatures (BS EN 1993-1-2, 2005). The ultimate load factor of 0.3 considered in the furnace fire test predicted the expected failure temperatures given by Eurocode 3 as 670 °C and 600 °C for yield strength and Young Modulus respectively, as shown in Fig. 7. However, the average recorded temperatures on composite cellular beams were, 699 °C on protected cellular B1, 726 °C on protected cellular B2 and 683 °C on protected cellular B3, when the average furnace temperature recoded was 922 °C.

The above observation leads to the conclusion that the lost rate of strength is slower than the lost of stiffness, decrease of Young Module. Thus, composite cellular beams main failure mode is web-post buckling, forming an S shape on the web between the openings as it ullustrared in Fig. 6. Closer observations on the symmetric protected cellular beam identified Vierendeel bending in combination with the web-post buckling.

4. Finite element modelling for fire conditions

The cellular steel beam sections and slab were modelled using the solid-brick element (Fig. 8) and heating element in order to add a temperature dependent mesh over the top of the structural mesh. Both the steel deck, as a bottom layer, and the reinforcing mesh as a layer within the concrete were included. Full interaction between composite slab, decking and cellular beams was insured, during the design and meshing stages. In order to simulate the tests as accurately as possible the beams were split into different areas. Different time/temperature curves were introduced to the model according to the average thermocouple reading recorded in the tests for the bottom flange, bottom web, upper web, upper flange, bottom layer of steel decking and concrete slab. Smeared cracking model was used for concrete which is characterised by the use of combining tension softening, tension cut-off and shear retention in order to analyse a concrete structure under loading.

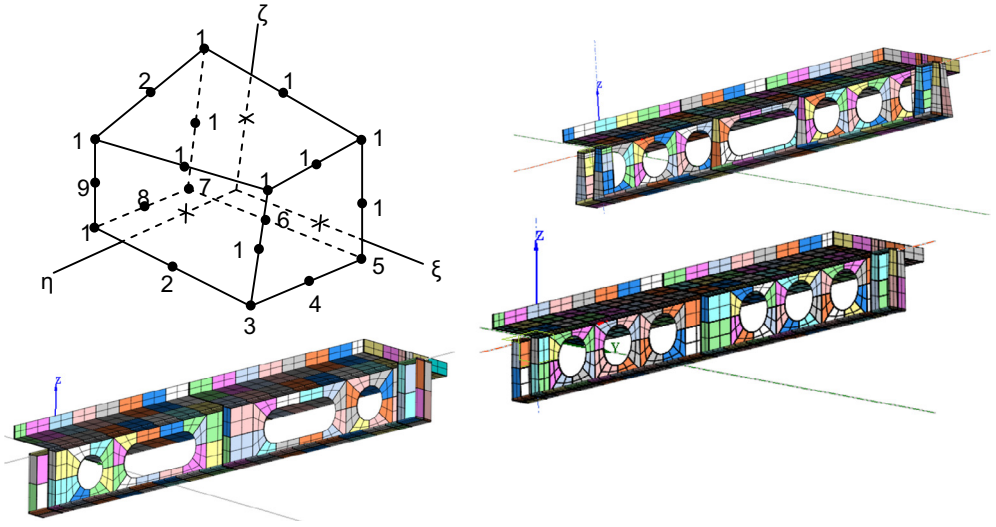

Fig. 8. Typical 20 nodes solid brick element and meshing of composite cellular beams.

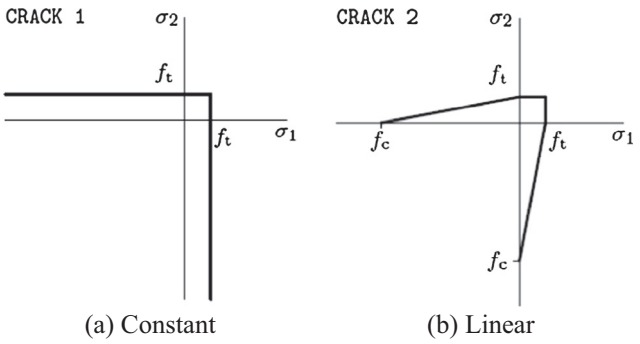

Fig. 9. Criteria for tension cut-off in smeared cracking.

Tension cut-off has one of two options to consider, either constant or linear performance under loading shown as shown in Fig. 9.

The thermal and mechanical properties of the concrete and steel are considered as temperature dependant and the relations suggested by the Eurocode 4 part 1–2 [13] were used throughout the work reported in this paper. For simplifying the models, the slab reinforcement and shear studs have not taken into account in the modelling. However, through the meshing process is ensured connection between composite slab and down stand cellular beams.

4.1. Fire load assignment

Based on the experimental observations on the furnace fire tests, the temperature distribution on the protected steel cellular beams is non-uniform. Although, the protected composite cellular beams were exposed on ISO-834 standard fire curve the resulted temperatures across the protected steel section have different profiles.

From the literature on researches preforming finite element analysis on protected cellular beams are presented two methods:

a. Adding on the original model, the protection material presenting it as an additional layer with thickness and properties for providing the required fire protection. This method requires creating an interface between the protection geometry and steel cellular beams, leading to complex finite element models.
b. The second method proposes the experimental recorded temperatures of each section part to be introduced on the finite element method [14].

The second methodology is adopted in this research for operating the finite element analysis of the protected composite cellular beams.

The reasons defending this are, for simplifying the finite element model, the supplier company did not provide the specific properties of the intumescent coating material and having an excellent set of experimental data is a great tool for creating an accurate finite element model.

4.2. Finite element analysis results

The simulation of the cellular beams were divided in different heated areas, top flange, top web, bottom web and bottom flange. Different time/temperature curves were introduced to each model according to the thermocouples readings in the fire tests for each part of the cellular beam section and lower surface of the steel decking. In this research study were used two approaches for the temperature distribution. On the first case all the section of the cellular beam, top flange, top web, bottom web and bottom flange were modelled using the average temperatures from the thermocouple readings. On the second case, the maximum-recorded temperatures were used for the top and bottom web, keeping the average recorded temperatures for top and bottom flanges.

The results obtained from the finite element analysis are presented in Fig. 10. It shows that the temperature deflection curves for each cellular beam, considering both cases for temperature distribution as described above. The two approaches of numerical modelling correspond reasonably well with the experimental results, having the results of the maximum web temperature distribution to be slightly closer. The approach of numerical modelling seems to agree well with the experimental fire tests. The failure mode that has taken place in the cellular beam 1 is due to the web posts buckling and Vierendeel bending as was seen in the fire test. At inial stage of loading, Vierendeel mechanism tends to develop starting due to the cellular geometry of specimen. Finally the beam fails by flexural web post buckling.

The axial stresses and Von Misses distribution at 66 min illustrate the critical parts of protected cellular B1, being in tension, as presented in the Fig. 10. Von Misses and axial stresses concentration are higher on the top web, around the openings, indicated by the green and orange colour respectively. This confirms the severe web-post buckling of top web due to the smaller size, thinner than the bottom web. In addition, the Vierendeel bending is located on openings 1, 2, 6 and 7 on the top web as shown in the axial stresses distribution in Fig. 10. There is no Vierendeel action on the elongated opening due to the transverse stiffeners.

For the B2, the stress concentration in the bottom part of the web around the elongated opening near the circular opening is in tension to a greater extent than the other parts of the web around openings and the stress concentration in the top part of the elongated openings is higher than the web post. From these observations and analysis, the failure mode of test B2 has clearly been the Vierendeel mechanism as expected associated with web post buckling. Furthermore, taking the axial stresses and Von Misses stresses distribution, Fig. 10, resulted from the average recorded temperatures approach; tensile forces, yellow colour in the figure, are mostly located in the top web with maximum on the elongated openings. The compression forces are indicated with green colour, which are dominating the beam along the span. Additionally, the tension located on the elongated opening on the bottom web reveals the failure mode for this protected beam is web-post buckling combined with Vierendeel bending. For B3, Von Misses and axial stresses concentration are higher on the top web, around the openings, indicated by the green and orange colour respectively, Fig. 10. This confirms the severe web-post buckling of top web due to the smaller size, thinner than the bottom web.

5. Analytical model

The failure mechanism for all the cellular beams was web-post buckling and Vierendeel mechanism. As an example, Fig. 11 illustrated the post web bucking failure of beam 1 after clearing the intumescent coating from that beam and expected failure happened when the critical temperature has been achieved.

From Fig. 11, we can see that the effective length subjected to buckling is different from beam-to-beam and therefore the shear buckling capacity of the web post at temperature θ, expressed in terms of longitudinal shear needs to be adjusted in comparison with the SCI approach design shown in Eqs (1)–(4)and more information are provided in Refs. [2,15].

For closely spaced openings, the effective length, l_{eff}, as an equivalent web post strut for a symmetrical section having circular and elongated circular openings is given as

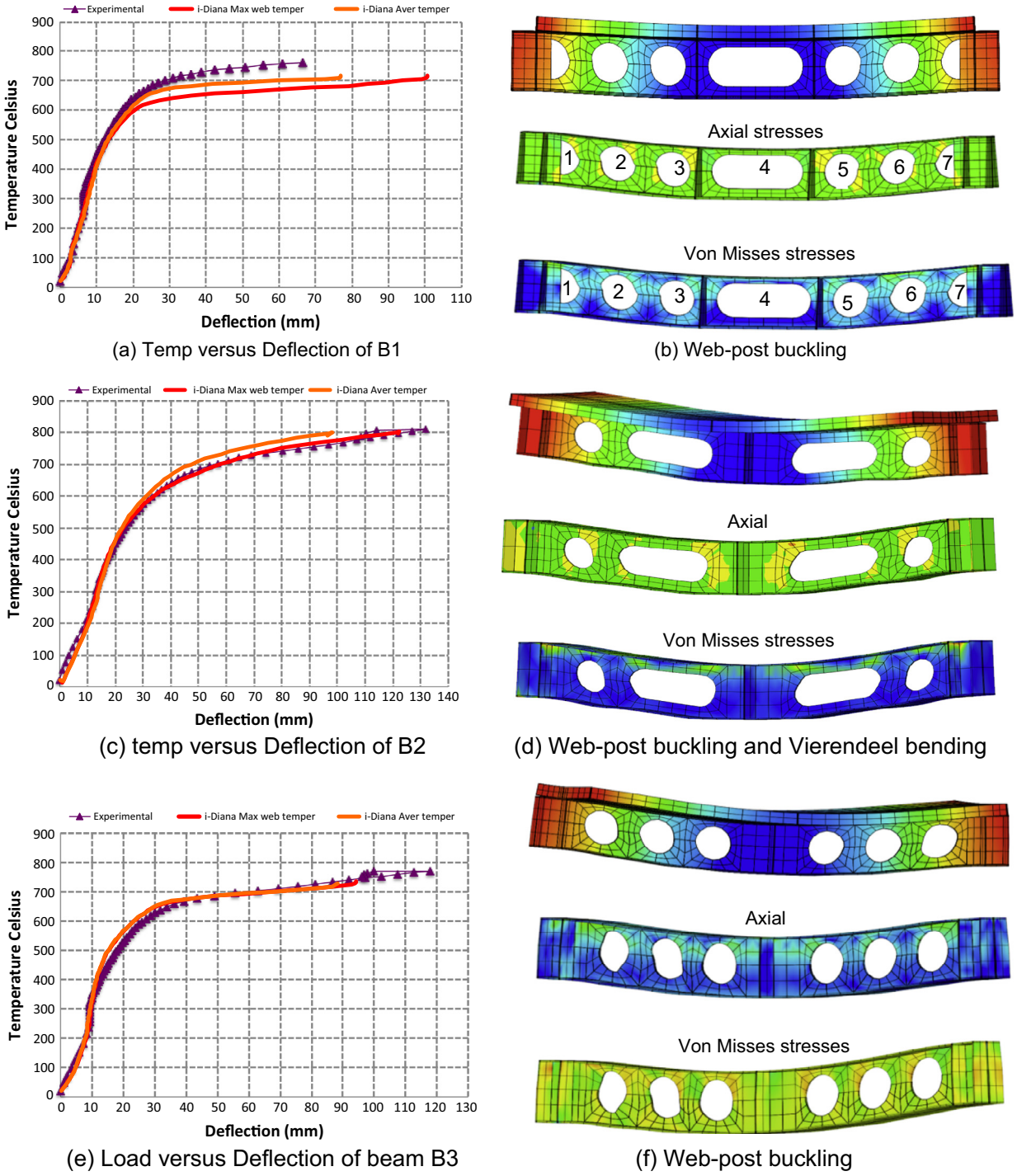

Fig. 10. Finite element results, beam deformation and failure mechanisms for protected beams.

$$l_{eff} = 0.5\sqrt{\left(S_0^2 + d_0^2\right)} \tag{1}$$

This value can be used for calculating the slenderness of the web post at the elevated temperatures (see Fig. 12). But in the asymmetric section where critical web thickness is nearly half of the other, effective length, shown as Fig. 12, considered to be applied by

$$l_{eff} = 0.25\sqrt{\left(S_0^2 + d_0^2\right)} \tag{2}$$

From this research project investigation It is recommended that the λ_θ can be adjusted in order to approach the practicality of the different cellular beams used in design constructions.

$$\lambda_\theta = \sqrt{\frac{f_{y,\theta}}{f_{E,\theta}}} \tag{3}$$

In here, $f_{y,\theta}$ is the design yield strength of steel at temperature θ.

$$f_{E,\theta} = \frac{\pi^2 E_\theta}{\lambda^2} \quad \text{and} \quad \lambda = \frac{\sqrt{12}\, l_{eff}}{t_{w,critical}} \tag{4}$$

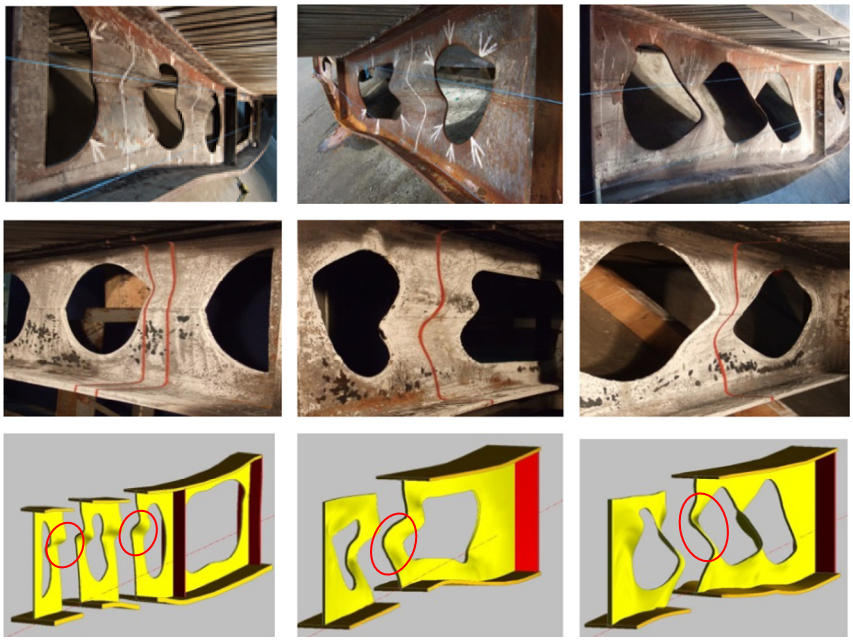

Fig. 11. Failure mechanism of (a) unprotected, (b) protected, (c) buckling lengths.

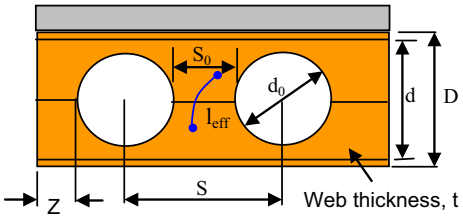

Fig. 12. Detail information of cellular beams.

where, $f_{E,\theta}$ is the elastic buckling stress at temperature θ and λ is the slenderness, determined on the basis of an effective length of an equivalent web post strut l_{eff}. $t_{w,critical}$ is the thickness of the web, in which, $l_{eff} = 0.5\sqrt{\left(S_0^2 + d_0^2\right)}$ for t_{wt}/t_{wb} = 1.0 for circular and elongated symmetric section $l_{eff} = 0.25\sqrt{\left(S_0^2 + d_0^2\right)}$ for $t_{wt}/t_{wb} \leqslant 0.6$ for circular and elongated asymmetric section.

6. Analytical analysis using Eurocode 3

Eurocode 3, EN 1993-1-2 [12], provides an equation for calculating the temperature increase $\Delta\theta_{a,t}$ of a protected steel member, in the case of uniform temperature distribution in a cross-section [16,17]. In Eq. (5), θ_t is the gas temperature, $\theta_{a,t}$ is the steel temperature, A_p/V is the section factor of the protected steel section, d_p fire protection material thickness, c_a, ρ_a, the specific heat and density of steel, c_p, ρ_p specific heat and density of the protection material and $\lambda_{p,t}$ the effective thermal conductivity of the fire protection material at time t

$$\Delta\theta_{a,t} = \left[\frac{\lambda_{p,t}/dp}{c_a\rho_a} \times \frac{A_p}{V} \times \left(\frac{1}{1+\emptyset/3}\right) \times (\theta_t - \theta_{a,t})\Delta t\right] - \left[\left(e^{\emptyset/10} - 1\right)\Delta\theta_t\right] \quad (5)$$

$$\emptyset = \frac{c_p\rho_p}{c_a\rho_a} \times d_p \times \frac{A_p}{V}, \quad \Delta\theta_{a,t} \geqslant 0, \ \Delta t \leqslant 30\ \text{s} \quad (6)$$

Intumescent coating is a thermal reactive material; consequently, its effective thermal conductivity does not have a fixed relationship with temperature. Thus, the fire exposure of intumescent coating is important [16]. In the paper of X.H et al. [17] the effective thermal conductivity of intumescent coating was computed using the inverse solution of Eq. (5) and experimental data from a test series of ten specimens [17,18]. This approach is being taken from DD ENV1331-4: 2002 [18].

The steel temperatures of protected steel section exposed to ISO 834 fire curve were calculated using Eq. (5). The thermal effective conductivity was taken as computed in papers X.H et al. [17]. The material properties of the intumescent coating are selected as density 1300 kg/m^3 and specific heat 1000 J/kg K. During the fire tests on the protected composite cellular beams, it was observed that the thickness of the thin film of the applied intumescent coating was changing, forming a thick char surrounding and insulating the steel beam cross-section from fire. Based on these observations the fire protection thickness and thermal properties materials were calibrated to be used in the calculations of the steel temperatures using Eq. (5). From Fig. 13 it can be concluded that the calculated

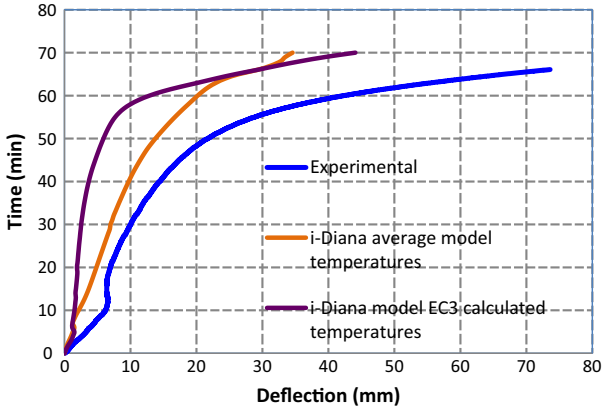

Fig. 13. Composite cellular beam 1 deflection results using Eurocode 3 method on i-Diana finite element software.

protected steel section temperatures by Eurocode 3 is relatively good in agreement with the experimental results. However, the equation can be improved by providing the temperature distribution of the cellular beam in other to adjust the thermal conductivity which could lead to better closer theoretical results.

7. Conclusions

This paper describes an experimental and analytical study of the behaviour of composite floor with protected and unprotected cellular steel beams in fire conditions conducted at the FireSERT, Ulster University; and it may be concluded that:

- Intumescent coating is the most effective fire protection material for steel cellular beams. The experimental results from the furnace fire tests of protected cellular beams compared to the results of tested unprotected cellular beams, have demonstrated that the recorded temperatures on the protected steel sections are less than the unprotected. Also, the deformation of the protected composite cellular beams is less crucial than the unprotected.
- The failure mechanism in the three protected composite cellular beams failed with the same manner as the unprotected but with a longer duration time and this is due to the insulation material used. The post web buckling lengths for cellular beams with different shapes and cross sectional dimensions are proposed.
- The numerical model is capable to simulate the mechanical behaviour of composite cellular beam sections protected at elevated temperature conditions with a relatively high accuracy.
- The Eurocode provided equation used in DIANA can provide quite good agreement with the experimental results when it is calibrated with the correct material specification of the intumescent coating used. The simplicity and versatility of the Eurecode with more additional data can be an attractive for application in fire resistance assessment in design and analysis situations.
- The research in Ulster University is taking step forward with the numerical modelling of intumescent coating protection for cellular steel beams using different load ratios and beam sledderness in order to provide the limit temperature for such of composite floor and improve the actual design rules.

Acknowledgements

The authors would like to thank the UK EPSRC (United Kingdom, Engineering and Physical Sciences Research Council) for providing the funding of this research (EP/F001525/1).

References

[1] K.F. Chung, T.C.H. Liu, A.C.H. Ko, Investigation on vierendeel mechanism in steel beams with circular web openings, J. Constr. Steel Res. 5 (57) (2001) 467–490.
[2] R.M. Lawson, J. Lim, S.J. Hicks, W.I. Simms, Design of composite asymmetric cellular beams and beams with large web openings, J. Constr. Steel Res. 6 (62) (2005) 614–629.
[3] K.D. Tsavdaridis, C. D'Mello, Web buckling study of the behaviour and strength of perforated steel beams with different novel web openings shapes, J. Constr. Steel Res. 67 (2011) 1605–1620.
[4] A. Nadjai, O. Vassart, F. Ali, D. Talamona, A. Allam, M. Hawes, Performance of cellular composite floor beams at elevated temperatures, Fire Saf. J. 42 (6–7) (2007) 489–497.
[5] A. Nadjai, C.G. Bailey, Sang-Hoon Han, O. Vassart, B. Zhao, M. Hawes, J.M. Franssen, I. Simms, Full-scale fire test on a composite floor slab incorporating long span cellular steel beams, Struct. Eng. 21 (2011) 18–25.
[6] A. Nadjai, N. Goodfellow, F.T. Kong, F. Ali, C. Seng-Kwan, Analysis of composite floor cellular steel beams in fire, J. Struct. Fire Eng. 1 (3) (2010) 161–175.
[7] Steel Construction Institute, Guidance on the use of intumescent coatings for the fire protection of beams with web openings, Document RT1085, Version 4, March 2007.
[8] Steel Construction Institute, Design of composite beams with large web openings, SCI publication P355, 2011.
[9] H. Van de Weijget, Protecting structural steel, Fire Saf. Eng. (2001) 16–19.
[10] P. Morris, Test of strength, Fire Saf. Eng. (2005) 17–20.
[11] E. Naili, A. Nadjai, F. Ali, Experimental and numerical modelling of cellular beams with circular and elongated web openings at elevated temperatures, J. Struct. Fire Eng. 2 (4) (2011) 288–300.
[12] Committee of European Normalisation CEN, Eurocode 3: design of steel structures, Part 1–2: general rules-structural fire design, ENV 1993-1-2. British Standards Institution, London, 1995.
[13] EN 1994-1-2, Eurocode 4 – design of composite steel and concrete structures – Part 1–1: Design for fire, CEN, Brussels, 2005.
[14] V.Y.B. Wong, I.W. Burgess, R.J. Plank, Experimental and analytical investigations of the behaviour of protected composite floor beams with web openings in fire, in: Conference Proceedings of Structures in Fire, SIF, 2010, pp. 366–373.
[15] SCI, Design of composite and non-composite cellular beams, P100, Ascot, 1994.
[16] R.P. Krishnamoorthy, C.G. Bailey, Temperature distribution of intumescent coated steel framed connection at elevated temperature, Conference Proceedings Nordic Steel 09, 2009, pp. 572–579.
[17] X. Dai, Y. Wang, G.C. Bailey, A simple method to predict temperatures on steel joints with partial intumescent coating fire protection, Fire Technol. 46 (1) (2010) 19–35.
[18] Committee of European Normalisation CEN, Test methods for determining the contribution to the fire resistance of structural members-Part 4: applied protection to steel members, DD ENC 13381-4, British Standards Institution, London, 2002.